JOURNAL OF PROPULSION AND POWER
Vol. 13, No. 2, March–April 1997

Power System Analysis of Multikilowatt Space/Planet Stations

George L. Kusic*
University of Pittsburgh, Pittsburgh, Pennsylvania 15261
and
Ronald C. Cull†
NASA Lewis Research Center, Cleveland, Ohio 44135

This paper describes a method to design modular power systems of multikilowatt size for satellite or planetary applications where the power source is periodic solar radiation. Energy for the eclipse period is from batteries or other storage mechanisms. Weight and efficiency of the electrical system are primary design parameters because the system must be rocket-boosted from Earth. Electrical losses are calculated for the network. Losses and weight of power converters are based on space application equipment. A three-module example operated at a specific load profile demonstrates how the method of the paper can be used for load scheduling and weight/power loss tradeoff.

Nomenclature

B_{im} = susceptance of transmission line im, S
C_{im} = capacitance line im to neutral, F
G_{im} = conductance of transmission line im, S
j = complex phasor operator
P_{im} = real power flow from bus i toward m, W
Q_{im} = reactive power flow from bus i toward m, W
R_{im} = resistance of transmission line im, Ω
V_i = node (or bus) line-to-neutral voltage, V
X_{im} = reactance of transmission line im, Ω
Y_{ii} = shunt admittance at bus i, S
Y_{im} = series admittance of transmission line im, S
$\angle\delta_i$ = phase angle of node i with respect to a reference at some point of the network, rad
ω = $2\pi f$, where f is the frequency in Hertz, rad/s

Introduction

MANY aerospace power systems include multiple sources with loads that must share use of the power generated. The design of these systems involves many considerations, such as minimum cost and mass, but maximum efficiency.

Unfortunately, design tools do not exist to fully investigate various options, especially in the early conceptual phases when design choices can have high leverage on the cost of the final system. Models that do exist tend to be either component models, systems modules that address only one or two attributes of the system, or custom design tools for a particular application. What is needed are integrated system engineering tools to allow the designer to perform trades between system components, architectures, and operations at the conceptual level.

To address this need, a program called Systems Engineering of Shared Resources has been started for aerospace power systems. The goal of the program is to develop a set of tools that can be used by designers and mission planners in the early design phases. The Aerospace Power Planning Program (APSPP) part of this program concentrated on identical modules and power conditioning elements.[1] A more general approach is to consider a mixture of different types of power modules such as expected for the International Space Station, which combines Russian Mir components with redesigned U.S. modules from Space Station Freedom.

There is the prospect of utilizing solar-energy Brayton or Sterling cycle systems with an ac generator output. Flywheel energy-storage mechanisms,[2] if used, have alternating current generators whose output power has to be incorporated into the power system.

A basic assumption of this paper is that the power system is distributed over a wide area, so that cable (or transmission line) weights and their electrical losses are both significant. This is in contrast to the case of a small satellite where power conversion from a photovoltaic panel is in close proximity to the power consumption electronics.

Power Transmission System

The single-phase power transmission cables service and return current conductors may be adjacent to each other as shown in Fig. 1a, separated as shown in Fig. 1b, or coaxial as shown in Fig. 1c. If the power is three phase, and assumed to be balanced, it can be described by an equivalent two-conductor circuit,[3] called a pi equivalent. The electrical resistance (ohms) caused by the length of the copper or aluminum conductors, and the capacitance and inductance caused by the length and spacing of parallel conductors,[4] determine the elements of the equivalent circuit. The pi approximation of Fig. 2 describes the voltage rise from input to open-circuited output caused by reactive cancellation between $2\pi fL$ and $1/(2\pi fC)$, where f is the line ac frequency $\omega = 2\pi f$. The pi approximation has an advantage over other equivalents in that it does not introduce a new node (or bus) at its center for power flow calculations.

Power flow through the transmission network is best analyzed in terms of real power (watts) and reactive power (volt-amperes-reactive, vars), because the electrical demand (load) on the network tends to be in watts when regulators maintain the output voltage, despite fluctuating supply. Phasor notation

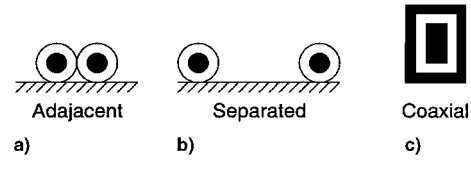

Fig. 1 Two-conductor transmission systems.

Received June 1, 1996; presented at the AIAA 31st Intersociety Energy Conversion Engineering Conference, Washington, DC, Aug. 11–16, 1996; revision received Oct. 12, 1996; accepted for publication Oct. 12, 1996.

*Associate Professor, Department of Electrical Engineering, 348 Benedum Hall.
†Power Systems Researcher, 21000 Brookpark Road.

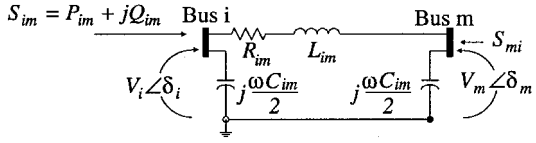

Fig. 2 Phasor power flow definitions for a transmission line from bus *i* to bus *m*.

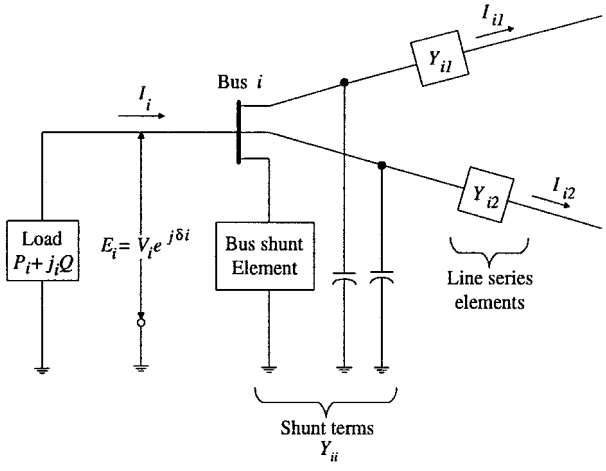

Fig. 3 Network for injections at bus *i*.

is shown on Fig. 2 for steady-state power flow on the pi equivalent:

$$Y_{im} = G_{im} + jB_{im} = 1/(R_{im} + j\omega L_{im}) = |Y_{im}|\angle\delta_{im}$$

A bus is a connection point of two or more power transmission lines. Each bus i on the network is connected to any number, $n \neq i$, of other buses. Total power $P_i + jQ_i$ of all lines connected to bus i is called an injection at the bus. The injection has negative components for real power consumption at lagging power factor. Network elements for power flow into bus i are shown in Fig. 3. Power flow into bus i is separated into real and imaginary components as

$$P_i = V_i \sum_{m \neq i}^{n} |Y_{im}|[V_i \cos\delta_{im} - V_m \cos(\delta_i - \delta_m - \delta_{im})] + V_i^2 \operatorname{Re}(y_{ii}^*) \quad (1)$$

$$Q_i = V_i \sum_{m \neq i}^{n} |Y_{im}|[-V_i \sin\delta_{im} - V_m \sin(\delta_i - \delta_m)] + V_i^2 \operatorname{Im}(y_{ii}^*) \quad (2)$$

where all buses may not be connected to bus i by transmission lines. Observe that power flow is a nonlinear function of the phase angle δ_m, and voltage V_m, at the buses. Therefore, iterative methods are necessary to solve simultaneously at all buses for the state vector $\boldsymbol{X} = (\delta_1, \delta_2, \ldots \delta_{n-1}, V_1, V_2, \ldots V_{n-1})^t$.

Because both real and imaginary power (load demand or supply) are specified at the buses, the n bus simultaneous equations are overdetermined, such that two slack variables have to be specified. This is the so-called slack bus, which is generally chosen to be the largest generator or power source on the network and is operated at fixed voltage with its phase angle as reference for the network.

Any power supply line frequency, $0 \leq f \leq 20{,}000$ Hz, is considered as a possibility for space power systems. The Newton–Raphson iterative method, compared to other algorithms, exhibits the most robust convergence to solve for the state $\boldsymbol{X}$ of the power system. In this method, the power mismatch at the $n-1$ buses for the kth iteration is the vector:

$$\begin{bmatrix} \Delta \boldsymbol{P} \\ \Delta \boldsymbol{Q} \end{bmatrix}^k = \begin{bmatrix} P_{f1} - P_1 \\ P_{f2} - P_2 \\ \vdots \\ P_{fn-1} - P_{n-1} \\ Q_{f1} - Q_1 \\ \vdots \\ Q_{fn-1} - Q_{n-1} \end{bmatrix} = \boldsymbol{b} - F(\boldsymbol{X}^k) \quad (3)$$

where the subscript f is a specified numerical value and $\boldsymbol{P}$ and $\boldsymbol{Q}$ are calculated from Eqs. (1) and (2), respectively.

The Jacobian is a $2(n-1) \times 2(n-1)$ matrix, which has to be inverted at each iteration k of the Newton–Raphson method to solve for the state $\boldsymbol{X}$:

$$\boldsymbol{X}^{k+1} = \begin{bmatrix} \boldsymbol{\delta} \\ \boldsymbol{V} \end{bmatrix}^k + \begin{bmatrix} \frac{\delta \boldsymbol{P}}{\delta \boldsymbol{\delta}}(X^k) & \frac{\delta \boldsymbol{P}}{\delta \boldsymbol{V}}(X^k) \\ \frac{\delta \boldsymbol{Q}}{\delta \boldsymbol{\delta}}(X^k) & \frac{\delta \boldsymbol{Q}}{\delta \boldsymbol{V}}(X^k) \end{bmatrix}^{-1} \begin{bmatrix} \Delta \boldsymbol{P} \\ \Delta \boldsymbol{Q} \end{bmatrix}^k = \begin{bmatrix} \boldsymbol{\delta} \\ \boldsymbol{V} \end{bmatrix}^k + \begin{bmatrix} J_1 & J_2 \\ J_3 & J_4 \end{bmatrix}^{-1} \begin{bmatrix} \Delta \boldsymbol{P} \\ \Delta \boldsymbol{Q} \end{bmatrix}^k \quad (4)$$

Each $(n-1) \times (n-1)$ quadrant J_i of the Jacobian contains only off-diagonal nonzero terms corresponding to transmission lines between buses. The partial derivatives of the Jacobian are calculated from Eqs. (1) and (2), and are re-evaluated at each iteration.

To keep the power flow computation general for any frequency, a minimum value $j\omega L_{im} = j0.0001$ of line reactance is retained. This results in var flows numerically negligible compared to real power flows and $\delta_i \sim 0.0$ for all angles for the dc case. Convergence of the Newton–Raphson iterations is still very quick (three or four iterations) with this approximation. A general power flow algorithm permits an aerospace engineer to compare different frequency power systems.

Power System Topology

For reliability purposes, for piece-by-piece assembly in space, and for interchangeability, modular topology is preferred for the power system. Before redesign in 1994, Space Station Freedom[4] had six power modules similar to module no. 1 shown in the one-line diagram in Fig. 4. The photovoltaic array, labeled PV in Fig. 4, uses a sequential shunt unit (SSU) to regulate its output voltage at bus no. 1 (encircled numeral). Each of the lines connecting encircled bus numbers in Fig. 4 is a pi section transmission line. Electrical loads for the entire power system are located on module no. 1 at bus nos. 21–28. The symbols α and β in Fig. 4 represent rotating mechanical joints with electrical slip-rings to point photovoltaic arrays. The α and β joints are treated as pure electrical resistance for power transmission. Other modules can ship (or receive) power to module no. 1 and the main loads by means of electrical ties to bus nos. 31 and 6. Module no. 2 shown in Fig. 5 is an ac module. It is a Brayton thermodynamic cycle 2-kHz, 440-Vac rotating machinery solar dynamic unit that has ac/dc power converters to supply power to bus no. 31. Converters are unilateral devices, which deliver scheduled amounts of power, regardless of fluctuations of the line voltage in module no. 2. The converters have scheduled power $P_{fk} + jQ_{fk}$ for Eq. (3). The solar dynamic source, bus no. 42, supplies all loads, battery charger/discharger unit (BCDU) demands at bus no. 35 and transmission line losses for the power flow computation on module no. 2. During eclipse time, the salt reservoir is a continuous heat source to provide full output power from the rotating machinery. Salt reservoir weight estimates used in the

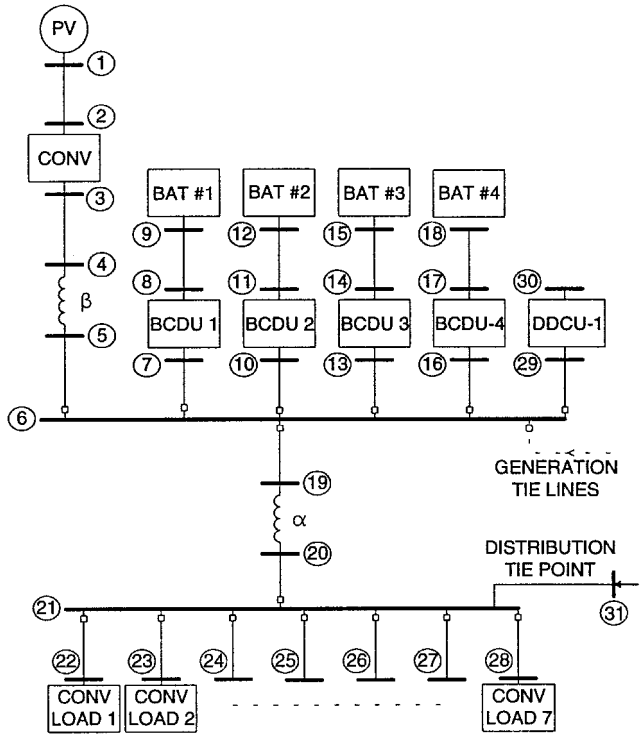

Fig. 4 Module 1 (150 Vdc, 31 buses, 22 lines).

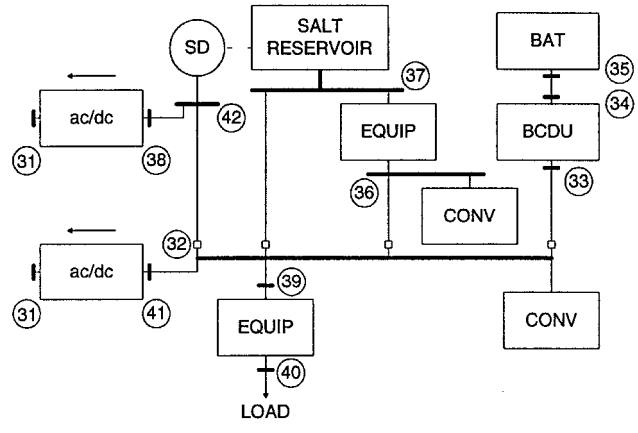

Fig. 5 Module 2 (2 kHz, 440 Vac, 11 buses, 8 lines).

program are valid for an eclipse time about one-third the orbit time. Module no. 3 in Fig. 6 is a 28-Vdc unit that requires dc/dc converters to step up its line voltage to transfer power to module no. 1 at bus no. 31. Converters shown in Fig. 6 at bus nos. 43 and 44 are unilateral. Rotating joints to point the PV array toward the sun are not shown.

Loads and Power Converters

Except for the transmission cables, all electrical losses must be removed by liquid coolant heat sinks and radiated into space. On Space Station Freedom, a decision was made to buffer all loads by 150- to 120-V dc/dc converters, which is not necessary when protective switchgear provides adequate isolation for faults.

Converters are a significant part of the electrical system. Several converters may be cascaded before the final power usage. The size, weight, and efficiency of large aerospace quality converters are estimated from component models[5] for ac/ac, dc/ac, and ac/dc converters. According to Ref. 5, an ac/dc converter with P_0 (kW) output, rated at P_r (kW), is estimated to require the control power P_c (kW):

$$P_c = 0.0447 P_r^{0.1} \tag{5}$$

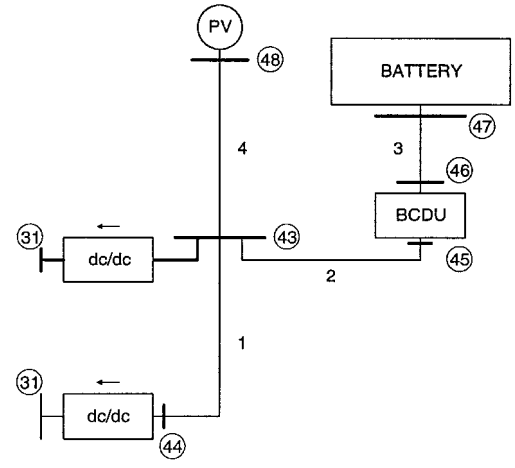

Fig. 6 Module 3 (8 buses, 4 lines).

The ac/dc converter contains a transformer, rectifier, and output filter with efficiencies $\varepsilon_t = 0.990$, $\varepsilon_r = 0.985$, and $\varepsilon_f = 0.995$, respectively. The overall ac/dc converter has the fractional efficiency ε:

$$\varepsilon = \frac{P_0}{P_c + P_0/(\varepsilon_t \varepsilon_r \varepsilon_f)} \tag{6}$$

Weights of these components, as well as heat sink or radiant enclosures, are estimated by similar expressions. For dc/dc converters, a few space-qualified units have been constructed to allow a logarithmic polynomial curve to be fitted to weight and efficiency vs power rating.[6] All converters are treated as P_0 scheduled output devices in the program.

The BCDUs shown on Figs. 4–6 are two dc/dc converters in the same electronics housing. One is a line power conditioner to charge the batteries, and the second in the reverse direction converts dc battery power to the line dc or ac voltage. Approximately one-sixth of the housing weight of two converters is saved by the BCDU single assembly. The measured BCDU charge/discharge efficiency curves[4] are used to compute losses. Battery efficiencies for charge and discharge are taken into account to calculate the total input energy (kilowatt hours).

The electrical loads on the modules are assumed to be specified as kilowatt demands on converters[7] connected to the buses of Figs. 4–6. Dummy converters (zero mass, 100% efficiency) are used for directly connected loads. Remote power controllers (RPCs) with solid-state switching taken from Table 1 (Ref. 8) are used in series with the converters with no. 12 American Wire Gauge wire to describe the secondary system connection.

To study the tradeoff possible between mass such as source mass, transmission system mass, and losses associated with power transmission, energy conversion and storage, the load time history is the predominating factor. For example, if there is negligible power demand during eclipse for an Earth orbit, then chemical or mechanical energy storage is very small.

Load Time Profile

Loads are treated as piecewise constant values for 1 min increments. It is assumed that a load scheduler program determines which load should be on at what time. The beginning of any time the spacecraft load changes is treated as a transition time. Figure 7 graphically shows the time histories of two loads and two types of battery charge profiles for a photovoltaic source spacecraft. A total of 11 transition times are shown on the figure, with variable duration periods between the transition instants. Two battery charge/discharge profiles are shown in Fig. 7. The average value of charge ramp for each time increment is treated as a piecewise constant value.

Table 1 Remote power controller weights for 120 Vdc

Type	Current rating	Weight, lb	Resistance, Ω
I	12	1.25	0.0268
II	25	3	0.0130
III	50	5	0.0065
IV	65	11.5	0.0047

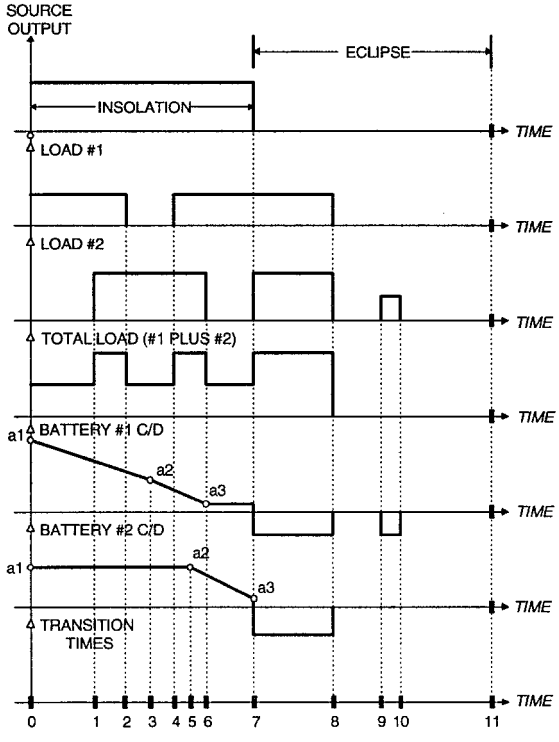

Fig. 7 Insolation, eclipse, and load cycle.

The performance computation starts at the onset of eclipse, point 7 in Fig. 7, and computes the kilowatt-hour drain on each battery during the eclipse interval to determine its equivalent state of charge (ESOC). Next the APSPP goes to time = 0, the onset of insolation, and computes the charge profile for each type of specified battery charge (points a1, a2, and a3 in Fig. 7) from the following types: type 0, flat charge for the entire insolation period; type 1, geosynchronous Earth orbit type of orbit with high initial rate of charge; and type 2, low Earth orbit type of orbit with flat rate of charge up to 90% of capacity, then taper to a 20% trickle value at the end of insolation.

Battery no. 1 in Fig. 7 has a type-1 charge profile, and battery no. 2 has a type-2 charge profile. Their discharges shown in Fig. 7 are a function of the power allocation program. The points marked a1, a2, and a3 for the batteries are computed from the ESOC at the beginning of insolation and maintained for the orbit.

800-W Spacecraft Example

To illustrate the impact of battery and load profiles, consider a spacecraft whose one-line electrical power system is shown in Fig. 6, except that the converter from bus no. 43 to bus no. 31 is not present. There is one dc/dc converter at bus no. 44. All lines are of no. 18 AWG and are 12, 10, 15, and 12 ft in length for lines L1, L2, L3, and L4, respectively.

The output of the SSU source controller is 128 Vdc and the power converter bus no. 44 reduces the high-system voltage to 40 Vdc. The weight and efficiency of the converter is calculated in the dc/dc converter subroutine.

The spacecraft has an orbit around the Earth with 55 min of insolation and 36 min of eclipse. The electrical load on the converter is constant at 305-W output from the converter. The converter efficiency is 80.4%, which causes a 379-W power demand at bus no. 44 of the electrical system.

The battery is NiHg with a storage capacity of 1050 W-h and weighs 13 kg. From among three optional methods of charging batteries, the battery is charged at a flat rate until it reaches 90% of charge, after which time the charge rate is tapered to a trickle level at the end of insolation. This is a type-2 charging. The energy balance to the battery includes fixed factors of 0.935 charge efficiency and 0.843 discharge efficiency, so that more energy enters the battery to account for the internal losses. There are also losses associated with the BCDU read from its efficiency curve. Figure 8 shows the battery energy cycle. BCDU discharge losses are 33 W at 0.92 efficiency and charge losses are 32 W during the flat period of charge.

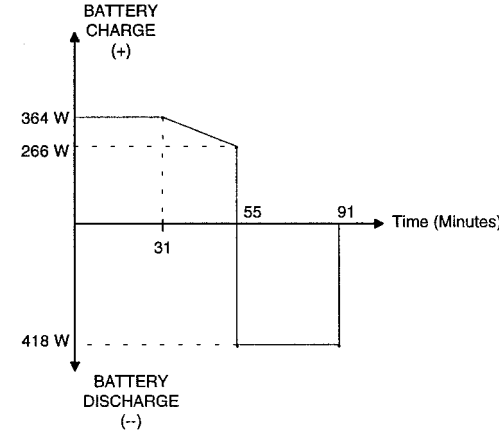

Fig. 8 Battery charge and discharge power for constant load.

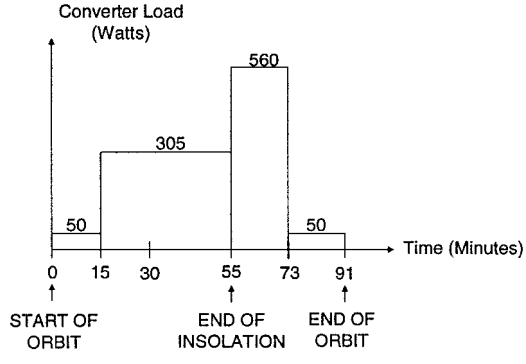

Fig. 9 Converter load time history.

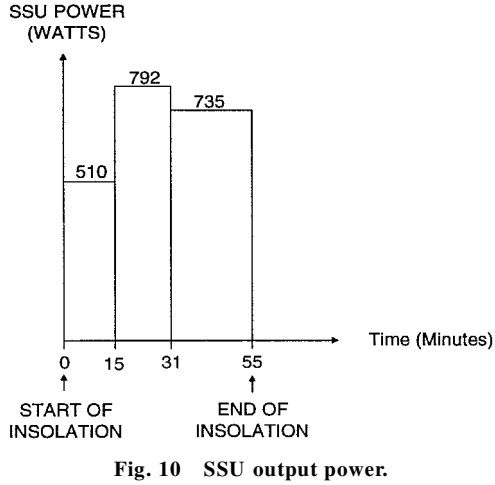

Fig. 10 SSU output power.

Transmission line losses are 13 W-h during insolation and 4 W-h during eclipse. The energy available from the SSU output terminals at bus no. 48 is 0.73 kW-h, but only 0.71 kW-h is utilized because the battery charge profile contains a taper region.

Next, the spacecraft is operated with a time-variable load on the output of the converter on bus no. 44 as shown on Fig. 9. The average load of Fig. 9 is 64 W-h less than the constant load.

During the eclipse period from minute 55 to minute 91, the battery through the BCDU supplies the power to the converter. Considering transmission cable losses, converter losses, and BCDU losses, the battery delivers 731 W during the time from minute 55 to minute 73. For the remaining eclipse time, minute 73 to 91, the battery delivers 113.2 W. The battery is assumed to have 15.7% internal losses during discharge, and so its true state of charge to begin the insolation period is lower than determined by power delivered to bus no. 45. The computed ESOC is 75.9% of the 1050 W-h capacity of the battery.

The output power of the SSU vs time as computed by the program is shown in Fig. 10. The SSU is not fully utilized because of the load and battery charge profile, and so it delivers only 0.63 kW-h to the system. Transmission line losses are 11 W-h during insolation and 7 W-h during eclipse.

Example of Design Perturbation

The three modules of Figs. 4–6 are operating as an interconnected system. Modules 1, 2, 3 have sources rated at 33, 32, and 28 kW, respectively. Module 3 is operated at 28 Vdc. Modules 2 and 3 continuously supply 20 kW of power to module 1 through the distribution tie bus no. 31. During insolation each module is recharging batteries and supplying loads through converters. ac module no. 2 employs 0.8 lagging power factor converters.

The peak load schedule for all buses in Table 2 is derived from converter efficiency estimates. Eclipse time load is 0.677 of the peak load for all three modules.

The transmission system cable lengths for module no. 1 are typical of Space Station Freedom. For module nos. 2 and 3 reasonable length estimates were used. During peak load, in all modules, the cables are operated near the current rating for Teflon®-insulated cable in vacuum conditions.[9] For an isolation time of 55 min and an eclipse time of 30 min, a performance summary of the three modules is given in Fig. 11. Energy

Table 2 Bus schedule at peak load condition

Bus	Load (kW)	Bus	Load (kW)
1	−20	25	2.02
2	0	26	4.90
3	0	27	5.69
4	0	28	2.53
5	0	29	6.51
6	0	30	0
7	0.464	31	No. 1 source
8	0	32	5.49
9	4.88	33	0.513
10	0.464	34	0
11	0	35	5.90
12	4.88	36	5.25
13	0.464	37	0
14	0	38	6.29
15	4.88	39	0
16	0	40	0
17	0	41	8.36
18	0	42	No. 2 source
19	0	43	3.16
20	0	44	3.16
21	0	45	0.514
22	0	46	0
23	6.54	47	5.92
24	6.66	48	No. 3 source

MODULE 1 RESULTS

	Weights (Kg)	Insol. % effic.	Eclipse % effic.
SOURCE	1608.00		
SSU	84.00	98.845	
BATTERIES	1266.06	93.500	84.300
BCDU s	171.75	92.000	92.000
TRANS NETWORK	243.12	96.908	99.271
RBI s	289.60		
DISTR NETWORK	3.94	100.000	100.000
RPC s	21.25	99.669	99.875
ALL CONVERTERS	289.55	93.284	93.005
RADIATORS	76.95		
TOTAL MODULE WT	**4054.22**		

SOURCE rated energy = 30.25 kW-Hrs, USED=29.48 kW-Hrs
BATTERY DOD = 27.6%
INSOLATION load = 30.55 kW, ECLIPSE av. load = 23.98 kW

LOSSES (kW-Hrs)	ORBIT	INSOLATION		ECLIPSE
TRANSMISSION LOSSES	= 1.584	= 1.478	+	.106
BCDU LOSSES	= 1.348	= 1.157	+	.191
BATTERY LOSSES	= 1.310	= .865	+	.444
CONVERTER LOSSES	= 4.052	= 2.773	+	1.280
SWITCHGEAR LOSSES	= .076	= .059	+	.018

MODULE 2 RESULTS

	Weights (Kg)	Insol. % effic.	Eclipse % effic.
SOURCE	2925.16		
SALT RESERVOIR	212.10		
BATTERIES	982.13	93.500	95.500
BCDU s	22.62	92.000	92.000
TRANS NETWORK	70.07	99.798	99.785
RBI s	162.90		
DISTR NETWORK	3.70	100.000	100.000
RPC s	1.70	99.939	99.967
ALL CONVERTERS	112.06	94.495	94.527
RADIATORS	34.96		
TOTAL MODULE WT	**4528.28**		

SOURCE rated energy = 48.53 kW-Hrs, USED = 46.59 kW-Hrs
BATTERY DOD = 0%
INSOLATION load = 31.81 kW, ECLIPSE av. load = 28.89 kW

LOSSES (kW-Hrs)	ORBIT	INSOLATION		ECLIPSE
TRANSMISSION LOSSES	= .096	= .059	+	.037
BCDU LOSSES	= .778	= .470	+	.308
BATTERY LOSSES	= .532	= .351	+	.181
CONVERTER LOSSES	= 2.000	= 1.279	+	.721
SWITCHGEAR LOSSES	= .012	= .008	+	.004

MODULE 3 RESULTS

	Weights (Kg)	Insol. % effic.	Eclipse % effic.
SOURCE	1364.36		
SSU	71.27	98.845	
BATTERIES	241.40	93.500	84.300
BCDU s	29.75	92.000	92.000
TRANS NETWORK	105.17	96.617	97.634
RBI s	90.50		
DISTR NETWORK	3.90	100.000	100.000
RPC s	.00	100.000	10.000
ALL CONVERTERS	113.62	95.000	95.000
RADIATORS	18.84		
TOTAL MODULE WT	**2038.82**		

SOURCE rated energy = 25.67 kW-Hrs, USED = 11.91 kW-Hrs
BATTERY DOD = 21.8%
INSOLATION load = 12.55 kW, ECLIPSE av. load = 6.86 kW

LOSSES (kW-Hrs)	ORBIT	INSOLATION		ECLIPSE
TRANSMISSION LOSSES	= .503	= .403	+	.100
BCDU LOSSES	= .787	= .457	+	.330
BATTERY LOSSES	= 1.109	= .342	+	.767
CONVERTER LOSSES	= .479	= .289	+	.189
SWITCHGEAR LOSSES	= .012	= .303	+	.198

Fig. 11 Summary of three modules for an orbit cycle.

losses in kilowatt-hours are tabulated for eclipse and insolation time periods. The solar dynamic source of module no. 2 continues to supply 31.81 kW of power during eclipse with energy from the salt reservoir. Almost full power from solar panel no. 1 is utilized. Only 46% of the available power from module no. 3 is used to allow a generation reserve for the interconnected modules. Transmission line losses are on the order of 5% for the photovoltaic modules (nos. 1 and 3) and 2% for the solar dynamic module.

To consider some design perturbations that result in an improved total system, module no. 3 is selected because it has a low system voltage. If the voltage of module no. 3 is increased to 150 Vdc, without changing the transmission cables, the BCDU weight decreases to 16.5 kg, the converters decrease to 63 kg, and the radiators decrease to 18 kg. The net saving from weights resulting from voltage level is 64 kg. Reducing the size of the transmission cables would reduce the weight an additional 86 kg (and the transmission losses would be less than the 1.26 kW-h shown in Fig. 11). The intermodule converters from module no. 3 to no. 1 could be replaced with solid-state switches to further reduce the total weight of module no. 3 to an improved value of approximately 1850 kg.

Concluding Remarks

This paper has considered the weight and efficiency of major elements in modular space/planetary power systems. When major elements are coupled by power flow for the system, it is possible to examine tradeoffs such as weight vs system voltage. The relative weight of source vs converters, such as for module no. 1 in Fig. 11, indicates to a system planner that three-phase ac should be evaluated as an alternative supply voltage. When second- and third-level dc/dc and dc/ac converters are included in the weight of the system, further advantages could be demonstrated for an ac system. The power flow and converter analysis may be used for energy balance studies when BCDU conversion and battery losses are calculated for an orbit cycle. A comparison of solar dynamic vs photovoltaic sources can include transmission network weight and converter weights to determine the best system.

NASA has developed a graphical user input program[10] to enter load time histories, the topology, and elements for modular aerospace power systems. All design procedures described here can be executed through the graphic interface.

Acknowledgment

This work was sponsored by NASA Grant NAG2-1691.

References

[1]Kusic, G. L., and Cull, R. C., "Power System Design Tool for Aerospace Applications," *Proceedings of the 29th Intersociety Energy Conversion Engineering Conference* (Monterey, CA), AIAA, Washington, DC, 1994, pp. 619–624.

[2]Post, R. B., Bender, D. A., and Merritt, B. T., "Electromechanical Battery Program at the Lawrence Livermore National Laboratory," *Proceedings of the 29th Intersociety Energy Conversion Engineering Conference* (Monterey, CA), AIAA, Washington, DC, 1994, pp. 1367–1373.

[3]Kusic, G. L., *Computer-Aided Power System Analysis*, Prentice–Hall, Englewood Cliffs, NJ, 1986.

[4]Hallinan, G. D., "Power System Description Document," Rockwell International Rocketdyne Div., Space Station Freedom Electric Power System Work Package WP-04, Contract NAS3-25082, DR:SE-02, Dec. 1992.

[5]Metcalf, K. J., "Lunar Power Management and Distribution Technology Assessment," Rockwell International Rocketdyne Div., Draft Report, Task Order 15, Contract NAS3-25808, Sept. 24, 1991.

[6]Scott, W. J., "Parametric Methods for dc/dc Converters," M.S. Thesis, Univ. of Pittsburgh, Pittsburgh, PA, 1994.

[7]Boley, S. B., "Reports, Electrical Power and Energy Status," Boeing Defense and Space Group, WP01 Space Station Freedom Program, DR SE19, D683-10238-A59, Huntsville, AL, Nov. 1993.

[8]Raley, J. B., et al., "Electrical Power System Trade Studies, Integrated Truss Assembly Secondary Power System Analysis," McDonnell Douglas, Huntington Beach, CA, Rept. MDC-H6433, DR CM-08.1, March 1993.

[9]Anon., "Wire and Cable Derating Data," NASA Military Standard 975J.

[10]Truong, L. V., "PC Software Graphics Tool for Conceptual Design of Space/Planetary Electrical Power Systems," 30th Intersociety Energy Conversion Engineering Conf., Paper 95-387, Orlando, FL, July 1995.